

## BLOCK DFE AND WINDOWING FOR DOPPLER-AFFECTED OFDM SYSTEMS

Luca Rugini<sup>1</sup>, Paolo Banelli<sup>1</sup>, and Geert Leus<sup>2</sup><sup>1</sup> DIEI, University of Perugia, Via G. Duranti 93, 06125 Perugia, Italy<sup>2</sup> Dept. of Elect. Eng., Delft University of Technology, 2628 CD Delft, The Netherlands

## ABSTRACT

Recently, a minimum mean-squared error (MMSE) block linear equalizer based on a band LDL<sup>H</sup> factorization has been proposed for equalization of orthogonal frequency-division multiplexing (OFDM) systems affected by Doppler spread. In this paper, we extend this approach towards two directions. First, we design an MMSE block decision-feedback equalizer (DFE) based on the band LDL<sup>H</sup> factorization. Both performance and complexity are analyzed. Second, we enhance the performance of the linear equalizer by means of receiver windows tailored to the band LDL<sup>H</sup> factorization approach. Simulation results show that the proposed techniques are effective in reducing the error floor caused by the intercarrier interference (ICI).

## 1. INTRODUCTION

OFDM is an effective technique that converts a time-invariant (TI) multipath channel in a set of parallel single-path channels, thereby facilitating the equalization [1]. When the channel is time-varying (TV), on the other hand, the orthogonality among the subcarriers is lost due to the presence of ICI [2][3]. Consequently, OFDM has mainly been adopted for TI channels. However, the request for communications at high frequency bands in high-mobility scenarios has spurred a renewed interest in equalization schemes for OFDM systems subject to significant Doppler spread [4]-[9].

To tackle this problem, recently, a low-complexity MMSE block linear equalizer (BLE) has been proposed in [10]. This BLE relies on the assumption that the ICI produced by faraway subcarriers can be neglected [6], and exploits a band LDL<sup>H</sup> factorization algorithm to reduce complexity, which is linear in the number of subcarriers [10]. However, the equalizer of [10] still has an error floor, mainly caused by the neglected ICI. In this paper we present two techniques that reduce this error floor while maintaining linear complexity. First, by using the MMSE approach of [11][12] we design a block DFE (BDFE) that incorporates the band LDL<sup>H</sup> factorization of [10]. Performance analysis and simulations show that the proposed BDFE outperforms the BLE of [10], while preserving exactly the same complexity.

The second technique we consider herein makes use of windowing [13] to reduce the sidelobes of the subcarrier spectrum, and hence the ICI. Receiver windowing has been previ-

ously proposed in [9] in order to minimize the neglected ICI. The scheme of [9] also adopts an ICI cancellation technique guided by an MMSE serial linear equalizer (SLE). In this paper, we modify the window design of [9] to consider block linear equalization. Simulation results illustrate that receiver windowing for BLE is more beneficial than for SLE when no ICI cancellation is adopted.

## 2. OFDM SYSTEM MODEL

We consider an OFDM system with  $N$  subcarriers. Assuming time and frequency synchronization, and employing a cyclic prefix length  $L$  greater than the maximum delay spread of the channel, the OFDM input-output relation for the  $i$ th OFDM symbol can be expressed by [4]-[9]

$$\mathbf{z}[i] = \mathbf{A}[i]\mathbf{a}[i] + \mathbf{u}[i], \quad (1)$$

where  $\mathbf{z}[i]$  is the  $N \times 1$  received vector,  $\mathbf{A}[i] = \mathbf{F}\mathbf{H}[i]\mathbf{F}^H$  is the  $N \times N$  frequency-domain channel matrix,  $\mathbf{H}[i]$  is the  $N \times N$  time-domain channel matrix,  $\mathbf{F}$  is the  $N \times N$  unitary FFT matrix,  $\mathbf{a}[i]$  is the  $N_A \times 1$  OFDM symbol that contains the frequency-domain data, and  $\mathbf{u}[i] = \mathbf{F}\mathbf{v}[i]$  is the  $N \times 1$  additive noise vector in the frequency domain, where  $\mathbf{v}[i]$  is the corresponding noise vector in the time domain. Assuming that  $N_A$  subcarriers are active and  $N_v = N - N_A$  are used as frequency guard bands, we can write  $\mathbf{a}[i]^T = [\mathbf{0}_{1 \times N_v/2} \mathbf{a}[i]^T \mathbf{0}_{1 \times N_v/2}]$ , where  $\mathbf{a}[i]$  is the  $N_A \times 1$  data vector. Assuming that the equalizer does not make use of the data received on the  $N_v$  virtual subcarriers, which contain little signal power, and dropping the block index  $i$  for the sake of simplicity, (1) becomes

$$\mathbf{z} = \mathbf{A}\mathbf{a} + \mathbf{n}, \quad (2)$$

where  $\mathbf{z}$  and  $\mathbf{n}$  are  $N_A \times 1$  vectors obtained by selecting the middle part of  $\mathbf{z}[i]$  and  $\mathbf{u}[i]$ , respectively, and  $\mathbf{A}$  is the  $N_A \times N_A$  matrix obtained by selecting the central block of  $\mathbf{A}[i]$ .

Throughout the paper, we assume that the channel matrix is known to the receiver. The topic of TV channel estimation, though important, is not considered herein and can be found elsewhere (see, e.g., [5][14]).

## 3. BANDED MMSE-BLE

Due to the TV nature of the channel,  $\mathbf{A}$  in (2) is not diagonal, but is nearly banded [6], and each diagonal is associated with a discrete Doppler frequency that introduces ICI. Hence,  $\mathbf{A}$  can be approximated by the band matrix  $\mathbf{B}$  obtained by selecting the main diagonal, the  $Q$  subdiagonals and  $Q$  superdiagonals, of  $\mathbf{A}$ . Thus,  $\mathbf{B} = \mathbf{A} \circ \mathbf{T}^{(Q)}$ , where  $\circ$  denotes the Hadamard (ele-

This work was partially supported by the Italian Ministry of University and Research under the project "MC-CDMA: an air interface for the 4th generation of wireless systems." Geert Leus was supported in part by NWO-STW under the VIDi program (DTC.6577).

ment-wise) product, and  $\mathbf{T}^{(Q)}$  is a matrix with lower and upper bandwidth  $Q$  [15] and all ones within its band. This approximation has been exploited in [10] to design a low-complexity MMSE-BLE, as expressed by

$$\tilde{\mathbf{a}}_{\text{MMSE-BLE}} = \mathbf{G}_{\text{MMSE-BLE}} \mathbf{z}, \quad (3)$$

$$\mathbf{G}_{\text{MMSE-BLE}} = \mathbf{B}^H (\mathbf{B}\mathbf{B}^H + \gamma^{-1}\mathbf{I}_{N_A})^{-1} = (\gamma^{-1}\mathbf{I}_{N_A} + \mathbf{B}^H\mathbf{B})^{-1}\mathbf{B}^H, \quad (4)$$

where the SNR  $\gamma = \sigma_a^2 / \sigma_n^2$  is assumed known to the receiver. By exploiting a band  $\text{LDL}^H$  factorization of the band matrix  $\mathbf{M} = \mathbf{B}\mathbf{B}^H + \gamma^{-1}\mathbf{I}_{N_A}$  (or equivalently of  $\mathbf{M} = \gamma^{-1}\mathbf{I}_{N_A} + \mathbf{B}^H\mathbf{B}$ ) the MMSE-BLE (3) requires approximately  $(8Q^2 + 22Q + 4)N_A$  complex operations [10]. The bandwidth parameter  $Q$  can be chosen to trade off performance for complexity. Taking into account the rule of thumb  $Q \geq \lceil f_b / \Delta_f \rceil + 1$  in [9], reasonable choices lie between  $Q=1$  and  $Q=4$ . Since  $Q \ll N_A$ , the computational complexity of the banded MMSE-BLE (3)-(4) is  $O(N_A)$ , i.e., significantly smaller than for other linear MMSE equalizers previously proposed, whose complexity is quadratic [8] or even cubic [7] in the number of subcarriers. In addition, as shown in [10], the complexity of the MMSE-BLE (5) is lower than for a non-iterative banded MMSE-SLE, i.e., the MMSE-SLE used to initialize the iterative ICI cancellation technique in [9]. We will now consider two ways to improve the performance of the banded MMSE-BLE.

## 4. BANDED MMSE-BDFE

### 4.1. Equalizer Design

In this section, we design a BDFE that exploits the low complexity offered by the band  $\text{LDL}^H$  factorization algorithm of [10]. To design the feedforward filter  $\mathbf{F}_F$  and the feedback filter  $\mathbf{F}_B$  (see Fig. 1), we adopt the MMSE approach of [11]. This approach minimizes the quantity  $MSE = \text{tr}(\mathbf{R}_{ee})$ , where  $\mathbf{R}_{xy} = E\{\mathbf{x}\mathbf{y}^H\}$  and  $\mathbf{e} = \tilde{\mathbf{a}} - \mathbf{a}$  (Fig. 1). We also impose the constraint that  $\mathbf{F}_B$  is strictly upper triangular, so that the feedback process can be performed by successive cancellation [12].

By the standard assumption of correct past decisions, i.e.,  $\hat{\mathbf{a}} = \mathbf{a}$ , the error vector can be expressed by  $\mathbf{e} = \mathbf{F}_F \mathbf{z} - (\mathbf{F}_B + \mathbf{I}_{N_A}) \mathbf{a}$ . By the orthogonality principle, it holds  $\mathbf{R}_{ee} = \mathbf{0}_{N_A \times N_A}$ , which leads to [11][12]

$$\mathbf{F}_F = (\mathbf{F}_B + \mathbf{I}_{N_A}) \mathbf{R}_{zz} \mathbf{R}_{zz}^{-1} = (\mathbf{F}_B + \mathbf{I}_{N_A}) \Lambda^H (\Lambda \Lambda^H + \gamma^{-1} \mathbf{I}_{N_A})^{-1}. \quad (6)$$

We now apply the band approximation  $\Lambda \approx \mathbf{B}$ , which by (4) leads to

$$\mathbf{F}_F = (\mathbf{F}_B + \mathbf{I}_{N_A}) \mathbf{G}_{\text{MMSE-BLE}}. \quad (7)$$

This result points out that the feedforward filter is the cascade of the low-complexity MMSE-BLE  $\mathbf{G}_{\text{MMSE-BLE}}$ , and an upper triangular matrix  $\mathbf{F}_B + \mathbf{I}_{N_A}$  with unit diagonal. To design  $\mathbf{F}_B$ , we observe that  $\mathbf{R}_{ee}$  can be expressed as  $\mathbf{R}_{ee} = (\mathbf{F}_B + \mathbf{I}_{N_A}) (\mathbf{R}_{zz} - \mathbf{R}_{zz} \mathbf{R}_{zz}^{-1} \mathbf{R}_{zz}^H) (\mathbf{F}_B + \mathbf{I}_{N_A})^H$ . After some calculations that also involve the matrix inversion lemma, we obtain

$$\mathbf{R}_{ee} = \sigma_n^2 (\mathbf{F}_B + \mathbf{I}_{N_A}) (\gamma^{-1} \mathbf{I}_{N_A} + \Lambda^H \Lambda)^{-1} (\mathbf{F}_B + \mathbf{I}_{N_A})^H. \quad (8)$$

To exploit the computational advantages given by the  $\text{LDL}^H$  factorization, we make the band approximation  $\Lambda^H \Lambda \approx \mathbf{B}^H \mathbf{B}$ , thus obtaining

$$\mathbf{R}_{ee} = \sigma_n^2 (\mathbf{F}_B + \mathbf{I}_{N_A}) (\gamma^{-1} \mathbf{I}_{N_A} + \mathbf{B}^H \mathbf{B})^{-1} (\mathbf{F}_B + \mathbf{I}_{N_A})^H. \quad (9)$$

Hence,  $\text{tr}(\mathbf{R}_{ee})$  can be minimized by using the  $\text{LDL}^H$  factoriza-

tion of  $\mathbf{M} = \gamma^{-1} \mathbf{I}_{N_A} + \mathbf{B}^H \mathbf{B}$ , expressed by  $\mathbf{M} = \mathbf{L} \mathbf{D} \mathbf{L}^H$ , and setting

$$\mathbf{F}_B = \mathbf{L}^H - \mathbf{I}_{N_A}. \quad (10)$$

By (10), (7), (4), and  $\mathbf{M} = \gamma^{-1} \mathbf{I}_{N_A} + \mathbf{B}^H \mathbf{B} = \mathbf{L} \mathbf{D} \mathbf{L}^H$ , we obtain

$$\mathbf{F}_F = \mathbf{L}^H \mathbf{G}_{\text{MMSE-BLE}} = \mathbf{L}^H \mathbf{M}^{-1} \mathbf{B}^H = \mathbf{D}^{-1} \mathbf{L}^{-1} \mathbf{B}^H. \quad (11)$$

Since  $\mathbf{B}$  is banded,  $\mathbf{L}$  is lower triangular and banded, and  $\mathbf{D}$  is diagonal, it turns out that the banded MMSE-BDFE is characterized by a very low complexity, as detailed in the following subsection.

### 4.2. Complexity Analysis

We now compute the number of complex operations necessary to perform the proposed banded BDFE. By means of (10) and (11), the soft output of the BDFE, expressed by  $\tilde{\mathbf{a}} = \mathbf{F}_F \mathbf{z} - \mathbf{F}_B \hat{\mathbf{a}}$ , can be rewritten as

$$\tilde{\mathbf{a}} = \mathbf{D}^{-1} \mathbf{L}^{-1} \mathbf{B}^H \mathbf{z} - (\mathbf{L}^H - \mathbf{I}_{N_A}) \hat{\mathbf{a}}. \quad (12)$$

Since  $\mathbf{B}$  is banded, we need  $(2Q+1)N_A$  complex multiplications (CM) and  $2QN_A$  complex additions (CA) to obtain  $\mathbf{y} = \mathbf{B}^H \mathbf{z}$ . The matrices  $\mathbf{L}$  and  $\mathbf{D}$  are obtained by band  $\text{LDL}^H$  factorization of  $\mathbf{M}$ . From [10],  $(2Q^2 + 3Q + 1)N_A$  CM and  $(2Q^2 + Q + 1)N_A$  CA are necessary to obtain  $\mathbf{M}$ . In addition, by the band  $\text{LDL}^H$  factorization algorithm of [10],  $(2Q^2 + 3Q)N_A$  CM,  $(2Q^2 + Q)N_A$  CA, and  $2QN_A$  complex divisions (CD) are required to obtain  $\mathbf{L}$  and  $\mathbf{D}$ . Then,  $\mathbf{x} = \mathbf{L}^{-1} \mathbf{B}^H \mathbf{z} = \mathbf{L}^{-1} \mathbf{y}$  can be obtained by solving the band triangular system  $\mathbf{L} \mathbf{x} = \mathbf{y}$ , which requires  $2QN_A$  CM and  $2QN_A$  CA [15], while  $\mathbf{D}^{-1} \mathbf{L}^{-1} \mathbf{B}^H \mathbf{z} = \mathbf{D}^{-1} \mathbf{x}$  requires  $N_A$  CD. To perform  $(\mathbf{L}^H - \mathbf{I}_{N_A}) \hat{\mathbf{a}}$ ,  $2QN_A$  CM and  $(2Q-1)N_A$  CA are required. Moreover,  $N_A$  CA are necessary to perform the subtraction between  $\mathbf{D}^{-1} \mathbf{L}^{-1} \mathbf{B}^H \mathbf{z}$  and  $(\mathbf{L}^H - \mathbf{I}_{N_A}) \hat{\mathbf{a}}$ . As a result, the proposed BDFE requires approximately  $(4Q^2 + 12Q + 2)N_A$  CM,  $(4Q^2 + 8Q + 1)N_A$  CA, and  $(2Q+1)N_A$  CD, for a total of  $(8Q^2 + 22Q + 4)N_A$  complex operations.

It is worth noting that, thanks to the banded approach, the proposed BDFE is characterized by exactly the same complexity of the BLE [10], which is linear in the number of subcarriers. Therefore, the proposed banded BDFE is less complex than other non-banded DFE schemes. Just to consider a few, the serial DFE [8] has quadratic complexity, while the complexity of the V-BLAST-like successive detection [7] is  $O(N_A^4)$ .

### 4.3. Performance Analysis

In this subsection we compare the mean-squared error (MSE) performance of the banded BDFE with that of the banded BLE [10]. By (9) and (10), it is easy to verify that

$$MSE_{\text{BDFE}} = \text{tr}(\mathbf{R}_{ee}) = \text{tr}(\sigma_n^2 \mathbf{L}^H \mathbf{M}^{-1} \mathbf{L}) \quad (13)$$

$$= \sigma_n^2 \text{tr}(\mathbf{D}^{-1}) = \sigma_n^2 \sum_{i=1}^{N_A} [\mathbf{D}^{-1}]_{i,i}. \quad (14)$$

Moreover, the MMSE-BLE can be obtained from the MMSE-BDFE by setting the feedback filter to zero. Thus, from (9) with  $\mathbf{F}_B = \mathbf{0}_{N_A \times N_A}$ , we obtain

$$MSE_{\text{BLE}} = \text{tr}(\mathbf{R}_{ee}) = \text{tr}(\sigma_n^2 \mathbf{M}^{-1}) = \sigma_n^2 \sum_{i=1}^{N_A} [\mathbf{M}^{-1}]_{i,i} \quad (15)$$

$$= \sigma_n^2 \sum_{i=1}^{N_A} \sum_{j=1}^{N_A} [(\mathbf{L}^H)^{-1}]_{i,i} [\mathbf{D}^{-1}]_{j,j} [\mathbf{L}^{-1}]_{j,i} \quad (16)$$

$$= \sigma_n^2 \sum_{i=1}^{N_A} [\mathbf{D}^{-1}]_{i,i} + \sigma_n^2 \sum_{i=1}^{N_A} \sum_{j=i+1}^{N_A} [\mathbf{D}^{-1}]_{j,j} |[\mathbf{L}^{-1}]_{j,i}|^2, \quad (17)$$

which is obviously greater than  $MSE_{\text{BDFE}}$  in (13)-(14). Hence, we expect that the bit error rate (BER) of the proposed BDFE will be lower than that of the BLE. This fact will be confirmed later by simulations.

## 5. BANDED MMSE-BLE WITH WINDOWING

Although the BDFE is characterized by improved performance with respect to the BLE, we still expect a BER floor, due to the band approximation of the channel matrix. The aim of this section is to investigate a time-domain windowing technique [9] that allows for a reduction of the band approximation error. Due to the lack of space, we will consider window designs for linear equalizers only.

Let us revisit the system model of (1). By applying an  $N \times 1$  time-domain window  $\mathbf{w}$  at the receiver before the FFT, the received vector can be expressed by [9]

$$\mathbf{z}_w[i] = \underline{\Lambda}_w[i] \underline{\mathbf{a}}[i] + \underline{\mathbf{n}}_w[i] = \underline{\mathbf{C}}_w \underline{\Lambda}[i] \underline{\mathbf{a}}[i] + \underline{\mathbf{C}}_w \underline{\mathbf{n}}[i] \quad (18)$$

where  $\underline{\Lambda}_w[i] = \mathbf{F} \underline{\Lambda}_w \mathbf{H}[i] \mathbf{F}^H$  is the frequency-domain windowed channel matrix, with  $\underline{\Lambda}_w = \text{diag}(\mathbf{w})$ ,  $\underline{\mathbf{n}}[i] = \mathbf{F} \underline{\Lambda}_w \mathbf{v}[i]$  is the windowed noise, and  $\underline{\mathbf{C}}_w = \mathbf{F} \underline{\Lambda}_w \mathbf{F}^H$  is the circulant matrix that represents the windowing operation in the frequency domain. By neglecting the data received on the guard bands, we have

$$\mathbf{z}_w = \underline{\Lambda}_w \underline{\mathbf{a}} + \underline{\mathbf{C}}_w \underline{\mathbf{n}}, \quad (19)$$

where  $\mathbf{z}_w$ ,  $\underline{\Lambda}_w$ , and  $\underline{\mathbf{C}}_w$  are the middle blocks of  $\mathbf{z}_w$ ,  $\underline{\Lambda}_w$ , and  $\underline{\mathbf{C}}_w$ , respectively, with size  $N_A \times 1$ ,  $N_A \times N_A$ , and  $N_A \times N$ , respectively. From the comparison between (19) and (2), it is clear that the main difference is the noise coloring produced by the windowing operation. Hence, by the band approximation  $\underline{\Lambda}_w \approx \mathbf{B}_w = \underline{\Lambda}_w \circ \mathbf{T}^{(Q)}$ , the MMSE-BLE becomes

$$\hat{\mathbf{a}}_w = \mathbf{G}_w \mathbf{z}_w, \quad (20)$$

$$\mathbf{G}_w = \mathbf{B}_w^H (\mathbf{B}_w \mathbf{B}_w^H + \gamma^{-1} \underline{\mathbf{C}}_w \underline{\mathbf{C}}_w^H)^{-1}. \quad (21)$$

### 5.1. Window Design

Our goal is to design a receiver window with two features:

- The approximation  $\underline{\Lambda}_w \approx \mathbf{B}_w$  should be as good as possible, and possibly better than the approximation  $\underline{\Lambda} \approx \mathbf{B}$ . This would reduce the residual ICI of the MMSE-BLE.
- The noise covariance matrix  $\underline{\mathbf{C}}_w \underline{\mathbf{C}}_w^H$  in (21) should be banded, so that the equalization can be performed by band LDL<sup>H</sup> factorization of  $\hat{\mathbf{M}}_w = \mathbf{B}_w \mathbf{B}_w^H + \gamma^{-1} \underline{\mathbf{C}}_w \underline{\mathbf{C}}_w^H$ .

We point out that, without the band approximation, the application of a time-domain window at the receiver does not change the MSE of the MMSE-BLE. This is why we adopt the minimum band approximation error (MBAE) criterion (a), which can be mathematically expressed as follows: Choose  $\mathbf{w}$  that minimizes  $E\{\|\mathbf{E}_w\|^2\}$ , where  $\mathbf{E}_w = \underline{\Lambda}_w - \mathbf{B}_w$  and  $\|\cdot\|$  is the Frobenius norm, subject to the energy constraint  $\text{tr}(\underline{\Lambda}_w^2) = N$ . (Equivalently,  $E\{\|\mathbf{B}_w\|^2\}$  can be maximized subject to the same constraint.) Note that this criterion is similar to the *max Average-SINR* criterion of [9]. Indeed, also in [9] the goal is to make the channel matrix more banded, in order to facilitate an iterative ICI cancellation receiver. Differently, in our case, we want to exploit the band LDL<sup>H</sup> factorization, and hence we also require the matrix  $\underline{\mathbf{C}}_w \underline{\mathbf{C}}_w^H$  in (21) to be banded. Since the  $N_A \times N_A$  matrix  $\underline{\mathbf{C}}_w \underline{\mathbf{C}}_w^H$  is the middle block of the  $N \times N$  matrix

$\underline{\mathbf{C}}_w \underline{\mathbf{C}}_w^H = \mathbf{F} \underline{\Lambda}_w \underline{\Lambda}_w^H \mathbf{F}^H$ , we impose the following sum-of-exponentials (SOE) constraint: The elements of the window  $\mathbf{w}$  should satisfy

$$[\mathbf{w}]_n = \sum_{q=-Q}^Q b_q \exp(j2\pi qn/N). \quad (22)$$

Indeed, when  $\mathbf{w}$  is a sum of  $2Q+1$  complex exponentials, the diagonal of  $\underline{\Lambda}_w \underline{\Lambda}_w^H$  can be expressed as the sum of  $4Q+1$  exponentials, and consequently, by the properties of the FFT matrix,  $\mathbf{F} \underline{\Lambda}_w \underline{\Lambda}_w^H \mathbf{F}^H$  is exactly banded with lower and upper bandwidth  $2Q$ . Obviously, the class of SOE windows includes some common cosine-based windows such as Hamming, Hann, and Blackman. The SOE constraint (22) can also be expressed by

$$\mathbf{w} = \tilde{\mathbf{F}} \mathbf{b}, \quad (23)$$

where  $\tilde{\mathbf{F}} = \sqrt{N} [\mathbf{f}_{N-Q}, \dots, \mathbf{f}_{N-1}, \mathbf{f}_0, \mathbf{f}_1, \dots, \mathbf{f}_Q]$  is obtained from the columns  $\{\mathbf{f}_i\}$  of the unitary IFFT matrix  $\mathbf{F}^H$ , and  $\mathbf{b} = [b_{-Q} \dots b_Q]^T$  is a vector of size  $2Q+1$  that contains the design parameters.

By applying the MBAE criterion, by the Appendix of [9], we obtain

$$E\{\|\mathbf{B}_w\|^2\} = \mathbf{w}^H (\mathbf{P} \circ \mathbf{A}) \mathbf{w}, \quad (24)$$

where  $\mathbf{P} = E\{\mathbf{H}\mathbf{H}^H\}$  contains the time-domain autocorrelation function of the channel, while  $\mathbf{A}$  is defined as

$$[\mathbf{A}]_{m,n} = \frac{\sin(\pi(2Q+1)(n-m)/N)}{N \sin(\pi(n-m)/N)}. \quad (25)$$

By maximizing (24) with the SOE constraint (23), the window parameters in  $\mathbf{b}$  are obtained by the eigenvector that corresponds to the largest eigenvalue of  $\tilde{\mathbf{F}}^H (\mathbf{P} \circ \mathbf{A}) \tilde{\mathbf{F}}$ . Note that this maximization leads to  $b_q = b_{-q}^*$ , and consequently the MBAE-SOE window is real and symmetric.

We remark that the window design depends not only on the selected  $Q$ , but also on the time-domain autocorrelation function of the channel contained in  $\mathbf{P}$ , and hence on the maximum Doppler frequency  $f_D$ . Therefore, even if we assume a specific Doppler spectrum (e.g., Jakes), the designed window will be different for each  $(f_D, Q)$ . Anyway, we will show that for reasonable values of  $f_D$  the designed window does not change so much. Consequently, a small set of windows can be designed and stored at the receiver, and chosen depending on  $(f_D, Q)$ .

### 5.2. Computational Complexity

In this subsection we show that the windowing operation produces a minimal increase in terms of computational complexity. In this computation, we neglect the complexity of the window design, which can be performed offline. For the same reason, we also neglect the computation of  $\underline{\mathbf{C}}_w \underline{\mathbf{C}}_w^H$ .

Since  $\underline{\mathbf{C}}_w \underline{\mathbf{C}}_w^H$  is circulant, its submatrix  $\underline{\mathbf{C}}_w \underline{\mathbf{C}}_w^H$  contains at most  $N$  different values. Moreover, due to the SOE constraint, only  $4Q+1$  entries are different from zero. Consequently, since  $\underline{\mathbf{C}}_w \underline{\mathbf{C}}_w^H$  is Hermitian, we need  $2Q+1$  CM to obtain  $\gamma^{-1} \underline{\mathbf{C}}_w \underline{\mathbf{C}}_w^H$ . Furthermore, approximately  $(2Q+1)N_A$  CA are required to sum  $\gamma^{-1} \underline{\mathbf{C}}_w \underline{\mathbf{C}}_w^H$  with  $\mathbf{B}_w \mathbf{B}_w^H$ , which is also Hermitian. In the absence of windowing, only  $N_A$  CA were necessary: Hence,  $2QN_A$  extra CA are required. In addition,  $N$  extra CM are needed to obtain  $\underline{\Lambda}_w \mathbf{H}$  in  $\underline{\Lambda}_w$ . We do not consider the complexity of the FFT, which should be performed also in the absence of windowing. As a result, the complexity increase of the banded MMSE-BLE due to windowing is roughly  $(2Q+1)N_A$  complex opera-

tions, for a total of  $(8Q^2 + 24Q + 5)N_A$  complex operations.

For the SLEs, the complexity increase is nearly equal than for the BLEs. Hence, the MMSE-BLE with windowing is less complex than the non-iterative MMSE-SLE with windowing.

## 6. SIMULATION RESULTS

In this section we compare by simulations the BER performance of the proposed techniques with that of the MMSE-BLE of [10], in order to understand the performance gain given by BDFE and by windowing. We consider an OFDM system with  $N=128$ ,  $N_A=96$ , cyclic prefix  $L=8$ , and QPSK modulation. We assume Rayleigh fading channels, an exponential power delay profile, and a Jakes' Doppler spectrum.

Fig. 2 illustrates the BER performance of the BDFE for different values of  $Q$  when  $f_D/\Delta_f=0.15$ . We remark that this value represents a high Doppler spread condition, since it corresponds to a mobile speed  $V=324$  Km/h for a carrier frequency  $f_c=10$  GHz and a subcarrier spacing  $\Delta_f=20$  kHz. From Fig. 2, we deduce that the performance improvement produced by the BDFE tends to increase for high values of  $Q$ . We also underline that the banded BDFE still has an error floor caused by the band approximation.

Fig. 3 shows the results of the MBAE-SOE window design when  $Q=1$  for different values of  $f_D/\Delta_f$ . In this case, since  $Q=1$ , there is a single amplitude parameter to be designed, expressed in Fig. 3 as the ratio  $2|b_1|/b_0$ . It is evident that for a large range of Doppler spreads the optimum ratio is close to the value 0.852, which is the ratio given by the Hamming window [13]. However, for very high Doppler spreads, the optimum ratio tends to decrease, i.e., more energy should be allocated to the cosine component. Fig. 4 presents the BER of the MMSE-BLE with SOE windowing when  $Q=1$  and  $f_D/\Delta_f=0.15$ . The best performance is obtained for the ratio  $2|b_1|/b_0=0.844$  given by the MBAE-SOE design. It should be pointed out that also other suboptimum SOE windows outperform the rectangular window (i.e., the case of no windowing), which can be considered as a degenerated SOE window with ratio  $2|b_1|/b_0$  equal to zero.

Fig. 5 exhibits the BER for some linear equalizers with windowing when  $Q=2$  and  $f_D/\Delta_f=0.15$ . As far as the BLE is concerned, the Hamming window, which is near-optimum for  $Q=1$ , outperforms the rectangular window. Anyway, the BER performance of the BLE with MBAE-SOE window is even better, thus confirming the goodness of our window design. Among the BLE approaches, the non-banded MMSE-BLE of [7] has the lowest BER, but its computational complexity is cubic instead of linear in the number of subcarriers. Fig. 5 also displays the BER of some non-iterative SLEs, with and without windowing, obtained from [8] and [9]. In the SLE case, windowing is less effective than for the BLE: The Hamming window is slightly worse than the rectangular window, and the Schniter window [9] is even worse. This indicates that for the SLEs windowing alone is not effective and should be coupled with iterative ICI cancellation techniques as in [9].

By Fig. 5, we can also note that the proposed banded MMSE-BLE with MBAE-SOE window outperforms the non-banded MMSE-SLE of [8], which has the lowest BER among the considered non-iterative SLE approaches. In addition, the proposed banded MMSE-BLE with MBAE-SOE window has linear complexity in the number of subcarriers, whereas the non-banded MMSE-SLE of [8] has quadratic complexity.

It is also interesting to observe that the application of MBAE-SOE windowing allows for a complexity reduction by simply reducing the parameter  $Q$ , without performance penalty. Indeed, by comparing Fig. 4 with Fig. 5, it is evident that the BLE with  $Q=1$  and MBAE-SOE windowing (i.e., that with  $2|b_1|/b_0=0.844$  in Fig. 4) outperforms the BLE with  $Q=2$  without windowing (i.e., that identified by rectangular window in Fig. 5). Besides, the complexity of the BLE with  $Q=1$  and windowing is roughly 46% of the complexity of the BLE with  $Q=2$  without windowing.

Fig. 6 depicts the shapes of the windows designed for  $Q=2$  and  $f_D/\Delta_f=0.15$ , used in Fig. 5. It is evident that the MBAE-SOE window and the Schniter window are very similar. The Schniter window, which is designed without the SOE constraint (23), produces an almost-banded noise covariance matrix. This means that the SOE constraint (23) does not exclude good windows. Moreover, it is interesting to note that for  $Q=2$  both the Schniter window and the MBAE-SOE window are very similar to the Blackman window [13]. We also remember that for  $Q=1$  the MBAE-SOE window and the Schniter window are similar to the Hamming window (at least for reasonable values of normalized Doppler spread). Although the Hamming and Blackman windows have been derived in a different context, we feel that this is not a merely coincidence. Indeed, many common windows, such as Hamming and Blackman, have been derived with the purpose of reducing the spectral sidelobes of the Fourier transform of the window [13]. Similarly, in our case, we want to mitigate the ICI outside the band of the channel matrix, and this ICI is caused by the spectral sidelobes of the Fourier transform of the window. However, in our scenario, the window design is also dependent on other factors, such as the Doppler spectrum and the maximum Doppler frequency.

## 7. CONCLUSIONS

In this paper, we have considered two techniques that reduce the ICI produced by Doppler spread in OFDM systems. First, we have presented a banded MMSE-BDFE that leads to improved BER performance with respect to a banded MMSE-BLE, with the same computational complexity. Second, we have considered a receiver window design for a banded MMSE-BLE, which outperforms, with lower complexity, some non-iterative MMSE-SLE approaches. Future work could investigate the joint design of windowing and banded MMSE-BDFE, as well as the effect of channel estimation errors.

## 8. REFERENCES

- [1] Z. Wang and G. B. Giannakis, "Wireless multicarrier communications: where Fourier meets Shannon," *IEEE Signal Processing Mag.*, vol. 17, pp. 29-48, May 2000.
- [2] M. Russell and G. L. Stüber, "Interchannel interference analysis of OFDM in a mobile environment," in *Proc. IEEE Veh. Tech. Conf.*, Chicago, IL, July 1995, pp. 820-824.
- [3] P. Robertson and S. Kaiser, "The effects of Doppler spreads on OFDM(A) mobile radio systems," in *Proc. IEEE Veh. Tech. Conf. Fall*, Amsterdam, The Netherlands, Sept. 1999, pp. 329-333.
- [4] I. Barhumi, G. Leus, and M. Moonen, "Time-domain and frequency-domain per-tone equalization for OFDM in doubly-selective channels," *Signal Processing*, vol. 84, pp. 2055-2066, Nov. 2004.

- [5] A. Gorokhov and J.-P. Linnartz, "Robust OFDM receivers for dispersive time-varying channels: Equalization and channel acquisition," *IEEE Trans. Commun.*, vol. 52, pp. 572-583, Apr. 2004.
- [6] W. G. Jeon, K. H. Chang, and Y. S. Cho, "An equalization technique for orthogonal frequency-division multiplexing systems in time-variant multipath channels," *IEEE Trans. Commun.*, vol. 47, pp. 27-32, Jan. 1999.
- [7] Y.-S. Choi, P. J. Voltz, and F. A. Cassara, "On channel estimation and detection for multicarrier signals in fast and selective Rayleigh fading channels," *IEEE Trans. Commun.*, vol. 49, pp. 1375-1387, Aug. 2001.
- [8] X. Cai and G. B. Giannakis, "Bounding performance and suppressing intercarrier interference in wireless mobile OFDM," *IEEE Trans. Commun.*, vol. 51, pp. 2047-2056, Dec. 2003.
- [9] P. Schniter, "Low-complexity equalization of OFDM in doubly selective channels," *IEEE Trans. Signal Processing*, vol. 52, pp. 1002-1011, Apr. 2004.
- [10] L. Rugini, P. Banelli, and G. Leus, "Simple equalization of time-varying channels for OFDM," to appear in *IEEE Commun. Lett.*, 2005.
- [11] N. Al-Dhahir and A. H. Sayed, "The finite-length multi-input multi-output MMSE-DFE," *IEEE Trans. Signal Processing*, vol. 48, pp. 2921-2936, Oct. 2000.
- [12] A. Stamoulis, G. B. Giannakis, and A. Scaglione, "Block FIR decision-feedback equalizers for filterbank precoded transmissions with blind channel estimation capabilities," *IEEE Trans. Commun.*, vol. 49, pp. 69-83, Jan. 2001.
- [13] F. J. Harris, "On the use of windows for harmonic analysis with the discrete Fourier transform," *IEEE Proc.*, vol. 66, pp. 51-83, Jan. 1978.
- [14] C. Sgraja and J. Lindner, "Estimation of rapid time-variant channels for OFDM using Wiener filtering," in *Proc. IEEE Int. Conf. Commun.*, Anchorage, AK, May 2003, vol. 4, pp. 2390-2395.
- [15] G. H. Golub and C. F. Van Loan, *Matrix Computations*, 3rd ed., Johns Hopkins Univ. Press, 1996.

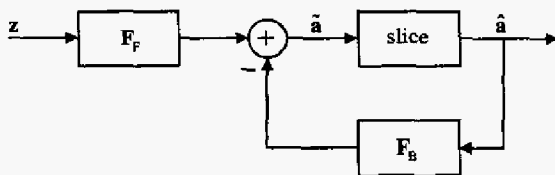


Fig. 1. Structure of the BDFE.

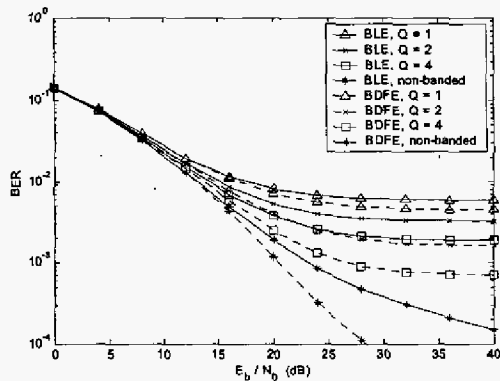


Fig. 2. BER comparison between MMSE-BLE and MMSE-BDFE ( $f_D/\Delta_f = 0.15$ ).

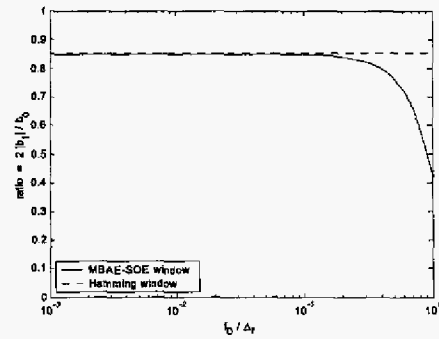


Fig. 3. MBAE-SOE window as a function of the normalized Doppler spread ( $Q=1$ ).

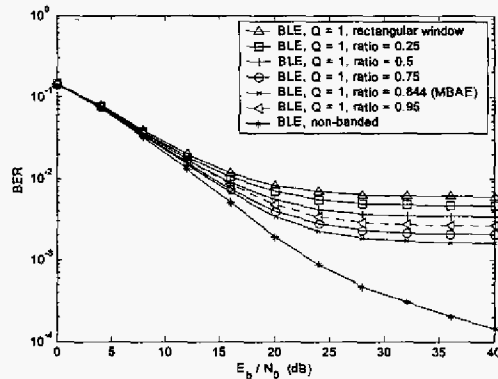


Fig. 4. BER of MMSE-BLE with different SOE windows ( $Q=1, f_D/\Delta_f = 0.15$ ).

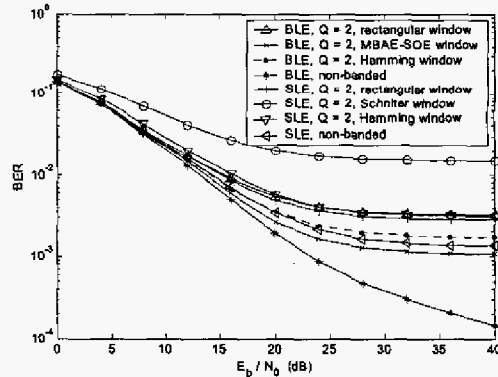


Fig. 5. BER of MMSE-BLE and MMSE-SLE with different windows ( $Q=2, f_D/\Delta_f = 0.15$ ).

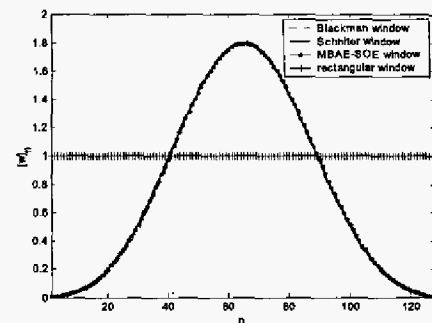


Fig. 6. Shape of different windows ( $Q=2, f_D/\Delta_f = 0.15$ ).